Ground Penetrating Radar Survey: Shankill Old Graveyard (Lurgan)

By: Alastair Ruffell, School of the Natural Built Environment, Queen's University, Belfast, BT7 1NN
a.ruffell@qub.ac.uk

Survey: Shankill Old Graveyard (Lurgan): Ground Penetrating Radar; Electro-magnetics

Contents[1]

1. Objective

To determine the presence of unmarked burials in areas with few or no visible grave markers.

2. Background

Historical (documentary) and anecdotal evidence suggests the presence of unmarked burials in Shankill Old Graveyard, likely due to, or associated with the Irish Famine (*syn:* Great Famine, Irish Potato Famine). From the author's experience, because the graveyard was situated at the northern limits of Lurgan through the mid 1800s, and close to the Cholera Hospital, makes this a likely location for burials at this time.

3. Context

Ground penetrating radar (GPR) has become the most popular geophysical method in the assessment of possible burials (Appendix 1), being more rapid than other methods (electrical resistance; seismic), less prone to magnetic interference (magnetometry [sometimes, gradiometry]) and sensitive to the detection of organic remains and ground disturbance.

So that the reader of this report may understand what is characteristic, some examples are provided, below.

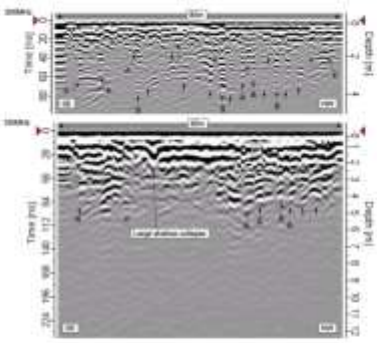

Above, two typical 2D GPR profiles from the Famine Graveyard (all unmarked, probably without any/substantial coffins present) at Omagh & Tyrone Hospital (in Ruffell et al, 2009). 200 MHz (upper image) is a suitable frequency for the detection of single inhumations, each labelled. A = shallow hyperbola from the top of a burial, crossed orthogonally; B: reverberation or 'ringing' below a grave,

[1] Fonts: main text: 12; background, figure captions: 10.5; Appendix: 9

caused by the radar wave bouncing up and down from an air-cavity; E: flat reflection, caused by surveying along the length of a grave. B: 100 MHz maybe too low a frequency for grave detection, but their presence here confirms the 200 MHz data, along with showing collapsed ground (often found above older burials).

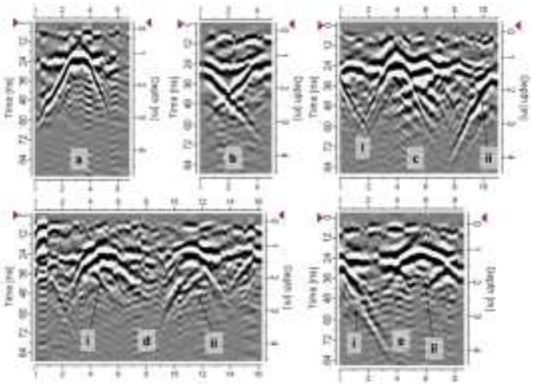

Above, typical, 2D individual 500 MHz GPR profiles over unmarked graves (Poor Ground, St. Brigid's. Drumkeeran, Co. Leitrim). a: hyperbola from the top of an inhumation; b: collapse above a grave; c: grave hyperbola, i) & ii) = edges of hyperbola ('side-swipe') from adjacent burials; d: burials with internal reflections, i) = material within grave, ii) = double-inhumation; e: (ii) = shallow grave with broad hyperbola and smaller second anomaly, i) = edge hyperbola, as in c). From: Ruffell & McAllister (2014).

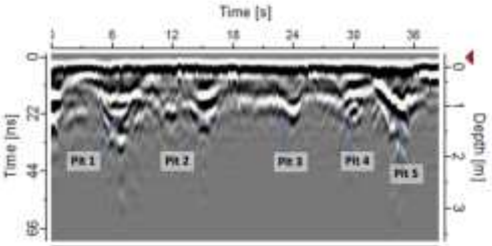

Above, example of 2D graveyard profile where collapsed ('Pit') ground is predominant (Friar's Bush, Belfast). From: Ruffell & McAllister (2014).

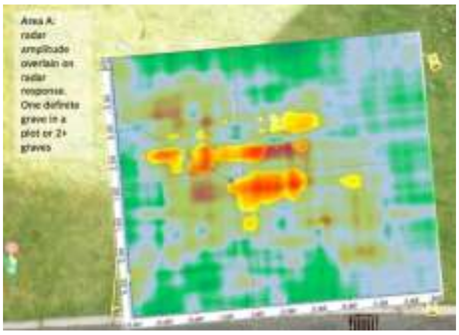

Above, common type of 3D GPR plot (slice through the ground at 1.3 m depth). Anahilt Church of Ireland, unpublished.

Above, example of 3D plot over one burial (top, head to left) and cut ground (centre). Cormac's Chapel, Cashel Cathedral, Co. Tipperary. Unpublished.

4. Methods

Two GPR systems were deployed to assess burials: 1) Mala 100 MHz and 500 MHz Pro-Ex system 2) GuidelineGeo 450 MHz High Dynamic Range system (latter is current, state of the art device and software).
Electromagnetics (CEIA compact detector) used to scan for metal items (grave goods, coffin handles).
To assess likely data quality, system 1) was used as a reconnaissance in August 2021, with Inspire drone for geolocation (Fig. 1). Data output was encouraging, so system 2) was used on 22-2-22 for both 2D and 3D surveys.
All profile locations were recorded using a Garmin E90 global navigation system (GPS) with barometer; cross-compared to the two in-built GPS receivers in the GPR antenna and control unit (provides a differential correction), further positioned using temporary ground markers imaged by orthogonal MavicPro drone (also with GPS). Data was viewed on site, in order to assess increasing survey limits or conducting more detailed work.

5. Areas Surveyed

Figure 1. Drone flight (August 2021, montage of 228 images, c/o Ben Rocke, QUB PhD student) with total area considered: some areas negated, surveys shown in Figure 2.

6. Results - Interpretations

Sixteen 2D lines over all three areas (A, B, C) were gathered in August 2021 and February 2022 (see above), followed by two grids in areas 1 and 2 (February 2022: 15 and 26 lines, respectively).

Figure 2. Location map of 2D (depth slice areas) and 3D (grid) surveys, with lines from Area A added (Fig 3). LDR = large deep reflector seen on Fig. 3, A3 and A4. Area 'north' considered in Conclusions. A, B, C – areas scanned in 2D; 1, 2 – grid locations.

6.1 Area A: Southern edge of Graveyard

Surveyed in both August 2021 and February 2022 as a possible location of Famine burials, ~10 isolated anomalies (Fig. 3), consistent with such were imaged at various locations, but not in the number or characteristics seen in other locations (see 'Context', above). A large, deep reflector (LDR) is observed where the southern graveyard wall has an inflection from SE – NW to ESE – WNW (LDR on Fig. 2), at 1 m depth adjacent to the wall and 0.5 – 0.75 m depth, some 4 m to the north, under the N-S path through the centre of the graveyard. This is consistent with a culvert.

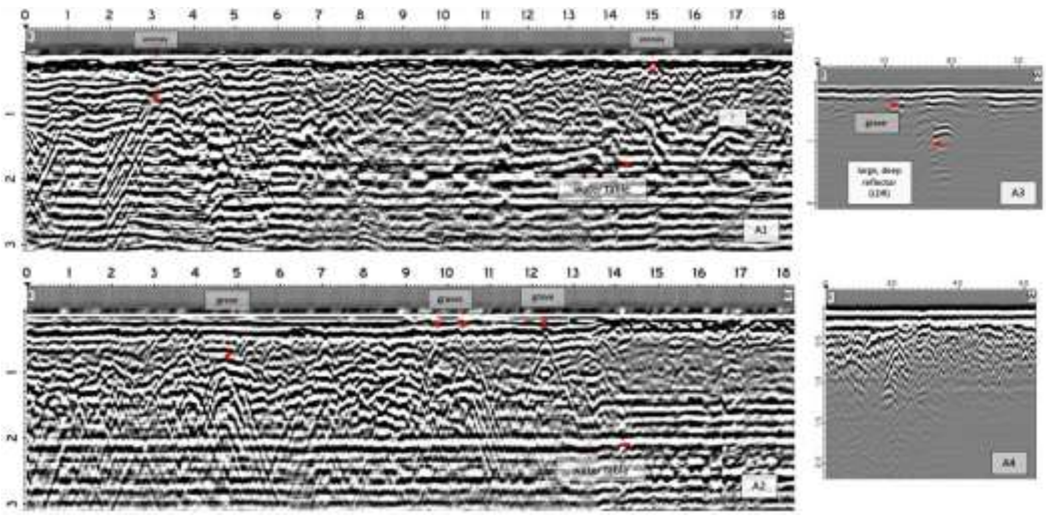

Figure 3, Area A 2D GPR lines. A1 and A2 = 450 MHz profiles, with scattered anomalies consistent with graves. A3 = 500 MHz and A4 = 100 MHz, showing the large deep reflector.

Figure 4. Area A Grid 1. A 3D grid was selected where anomalies were noted on 2D profiles: a 3D grid has the capability to resolve numerous graves and their length/width, more accurately than 2D profiles. Only two (adjacent) anomalies that are consistent with poorly-defined graves were imaged. Inset: grid on real-time imagery.

6.2 Area B: Centre (N-S) of Graveyard

Surveyed in 2D in February 2022, this area was also identified by staff as a possible location for Famine burials. Reconnaissance, N-S and E-W 2D lines were gathered over the area, three of which are shown in Figure 5. Like Area B, isolated graves were imaged east of headstones, the centre portion of Area B is devoid of graves (Line B2 on Fig. 6), making this unlikely to be Famine Ground. No 3D grid was surveyed as a result.

Figure 5. Area B line map of the selected profiles, seen in Fig. 6.

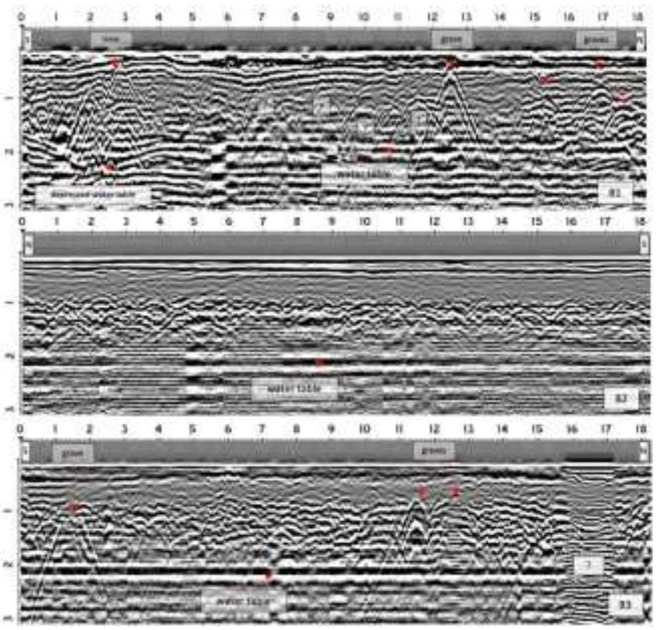
Figure 6. Area B 2D profiles (on Fig. 5), showing isolated burials to east and west. Flat reflectors on Line B3 are consistent with a rock or concrete slab (e.g. headstone, inspection cover). Note the absence of hyperbolas on Line B2 (centre of Area B).

6.3 Area C: North-eastern Corner of Graveyard

This area was surveyed for similar reasons as A and B, being largely devoid of headstone markers. Figures 7 and 8 confirm a similar pattern to the other areas, with isolated graves and one exception – a portion of disturbed ground occurs to the south-west (SW) of Area C. This is picked out on Figure 8 as an area of note, if still equivocal in nature.

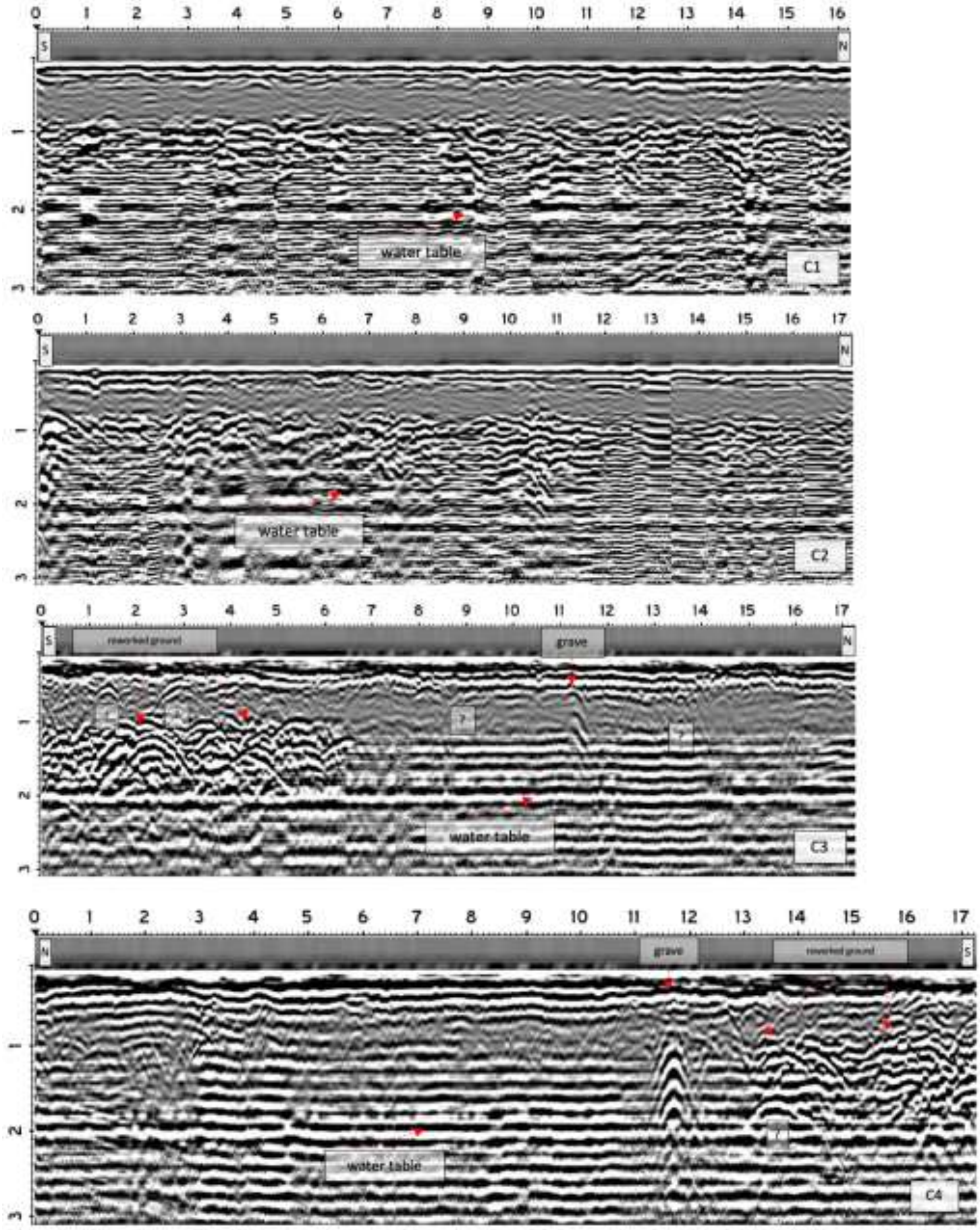

Figures 7 and 8. Selected 2D profiles (450 MHz) across Area C, showing isolated burials and the disturbed ground to the SW: hence enlarged Line C4 (Figure 8).

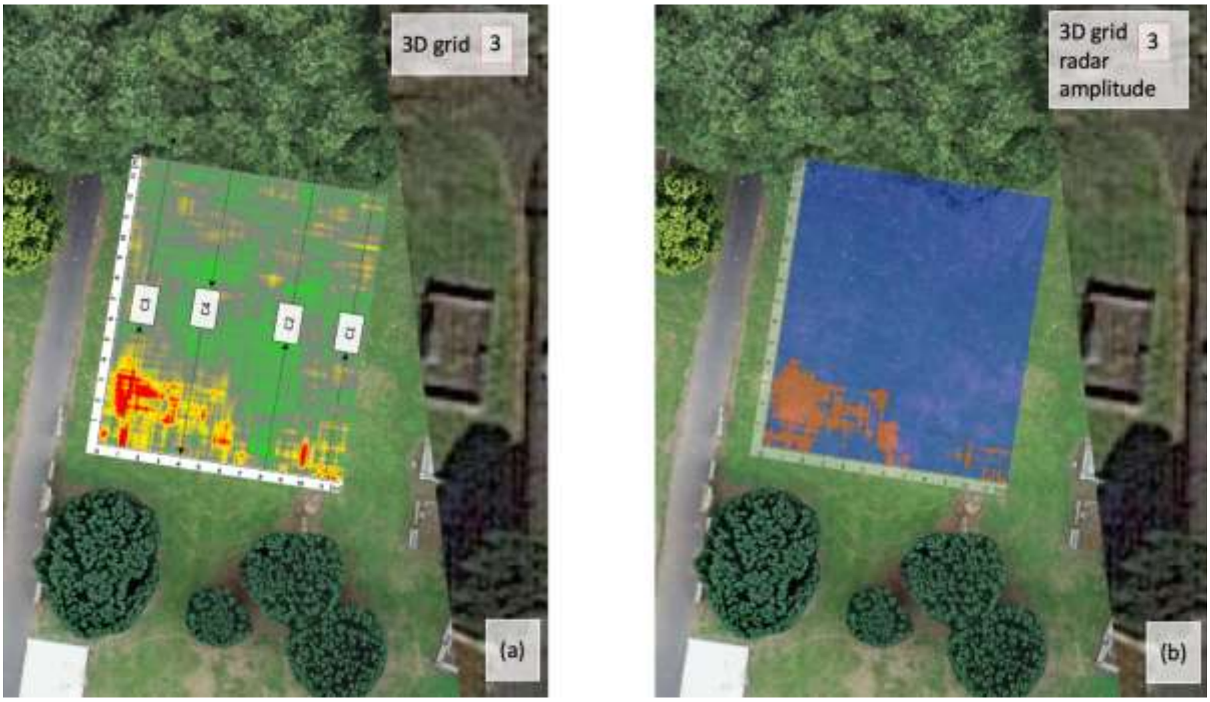

Figure 9. Area C Grid. (a) is unprocessed, showing disturbed ground to the SW and a square anomaly (without extant burial) to the east (southern section of Line C1, Fig. 7): this maybe a buried grave-plot, unused, decayed or with coffin slip. E-W elongate (yellow) areas maybe burials or dug locations. (b) is processed to remove all but the highest radar amplitudes (see Comina et al, 2020; Kelly et al, 2021), confirming the presence of disturbed ground in this area: anomalies consistent with burials (Fig. 7) occur in this ground.

7. Conclusions

As would be expected in any survey of burial grounds, numerous anomalies occur throughout the areas surveyed in Shankill Old Graveyard: none however are consistent with other surveys of Irish Famine burial grounds (see Context, above), being isolated and with the hyperbolas and side-swipe more common with coffin burials. A probable culvert is identified, running north to south, in the middle of Area A. The only ground with the highest likelihood of having numerous burials is the SW corner of Area C (Fig. 9).

Where are the recorded Irish Famine burials? These possibilities are considered:

1. They are not in one consistent area, scattered through the graveyard. This would be consistent with the results of this survey, but not with many other Famine burial grounds.
2. Ground conditions are such that insufficient contrast between soil and burials exists to be successfully resolved on GPR: this is inconsistent with the good imaging of graves elsewhere in the grounds surveyed here, unless all Famine graves were without coffins and/or without significance quantities of added lime (common practice during the Famine, making a good radar target). This would mean that many of the areas surveyed appear to be without burials, but do indeed have them: this is possible, but not encountered by the author before.
3. A portion of Famine Ground exists in the SW corner of Area C, Grid 3.
4. The above (3), and/or the vegetated area to the north of the surveyed ground is the main location of Famine ground: much of the northern area has spoil from railway

workings and irregular vegetation: this would need to be cut back for the least compromised ground to be surveyed.

8. Acknowledgements

The surveys were kindly funded by the Department for Communities: Historic Environment Division through the Historic Environment Fund; and the Armagh City, Banbridge and Craigavon Borough Council and The National Lottery Heritage Fund through the Lurgan Townscape Heritage Scheme (Lurgan TH). David Weir (Lurgan TH, Armagh City, Banbridge, & Craigavon Council) and Isobel Hylands (Friends of Shankill Graveyard) instigated this work and assisted on site. The help of Queen's University students Lauren Carberry-O'Neill, Lauren Gill, Ben Rocke, Oran Somers, Lisa White was essential. Mike Langton of GuidelineGeo loaned the 450 MHz HDR radar system.

9. References

Comina, C., et al. 2020. Geophysical surveys over and inside Tobiotsuka Kofun – Okayama prefecture. Journal of Archaeological Science: Reports. 30., https://doi.org/10.1016/j.jasrep.2020.102256

Kelley, T.B. et al. 2021. A novel approach to 3D modelling ground-penetrating radar (GPR) – A case study of a cemetery and applications for criminal investigation. Forensic Science International, doi: 10.1016/j.forsciint.2021.110882.

Ruffell, A., McCabe, A., Donnelly, C. & Sloan, B. 2009. Location and assessment of an historic (15-60 years old) mass grave using geographic and ground-penetrating radar investigation. NW Ireland. *Journal of Forensic Sciences,* **54**, 15-26. doi.org.10.1111/j.1556-4029.2008.00978.x

Ruffell, A. & McAllister, S. 2014. A RAG system for forensic and archaeological searches of burial grounds. *International Journal of Archaeology*, **3**, 1-8. DOI: 10.11648/j.ija.s.20150301.11

10. Appendix

GPR – How the Method Works

GPR uses the transmission and reflection of radio waves (typically 25 to 2GHz) in imaging the subsurface. Radar waves, introduced in the ground, may reflect back to surface when they intersect objects or surfaces of varying dielectric permittivity. Thus a GPR system requires a source antenna and receiving antenna (built to measure the same central frequency). The transmitting antenna generates a pulse of radio waves that the receiver detects at a set time interval: the longer the time interval, (potentially) the deeper the waves will have travelled into the ground (or to a nearby surface object) and back again. When the ground has a slow radar wave velocity, so a buried object may appear deeper than in ground with a fast transmissive velocity. As the antennas pass over discrete objects with different dielectric properties to the surrounding medium (boulders, pipes, coffins, trenches), they may generate hyperbolae, or arc-like reflections, or depressions. Radar waves also travel horizontally from the transmitting antenna, which in open ground simply dissipate with distance. However, in areas with upstanding structures, especially those that have a significant dielectric contrast to their surroundings, interference from such surface objects can create artefacts on the radargram. When such isolated objects (powerlines, telegraph wires, metal poles, trees) are passed during a traverse, a series of hyperbolae may be generated that appear like a subsurface object but are simply out-of-plane reflections. Radar antennae are commonly elongate (bow-tie shape), generating radar waves in a widening arc from their long axis. Thus when moved in parallel to the antennae axis, the radar waves may reflect from a larger subsurface area in front and behind the antenna, (the so-called footprint) than when moved with the antennae at right angles to survey direction. Antennae may be shielded with radio-wave attenuating materials (e.g. aluminium) that reduce such out-of-plane interference. Unlike other forms of electromagnetic radiation used in geophysics, radio waves have far higher rates of attenuation, and thus penetration and reflection depths are typically low, but horizontal accuracy is high, coupled with rapid, real-time results, unlike all other geophysical techniques bar metal detectors and magnetometer raw data. The receiving antenna has either electronic or fibre-optic link to a recorder that converts incoming radio waves to digital format and displays these graphically as wavelets. As the transmitter-receiver array is moved, so these wavelets are stacked horizontally to produce a radargram, a kind of x-ray slice into the Earth, but recorded in the time taken for radar waves to penetrate and reflect, as opposed to real depth. The speed of radio wave propagation is determined by the makeup of the transmitting medium: in this case the speed of light and dielectric permittivity. Magnetic properties can also influence radar wave speed. Changes in dielectric permittivity can cause radar wave reflection, without which GPR profiling would be impossible. Radar wave attenuation, or signal loss is extreme in conductive media such as seawater, clays (especially hydrous) and some leachate. GPR has good depth penetration (tens to hundreds of metres) in ice (with minor fracturing/interstitial water), hard rocks like limestone and granite and clay-poor quartz silts or sands. Vertical resolution *vs.* depth penetration is of major concern when choosing antenna frequency. Low frequencies (15-50MHz) achieve deep penetration with poor horizontal resolution in the received signal, due to the long wavelength. High frequencies (500-1000MHz) show high resolution with weak penetration (centimetres to metres). Low-frequency antennae are large (a few metres long), high frequency antenna are small (tens of centimetres). Again, this can influence the use of the method, as deeply-buried targets in enclosed spaces are virtually impossible to survey.

As with all geophysical methods, some intelligence concerning the likely size and makeup of the target is useful: where unknown or questioned, then a range of antennas should be used, and in very poorly understood locations, with other geophysical and invasive techniques (Blunderbuss Approach). Moisture contents influence radar wave velocity because in homogenous media porosity has a direct relationship to dielectric permittivity. Thus dry sand will allow increased wave propagation: sand with high freshwater content will give improved vertical resolution. A problem with unshielded antennas is the effect of 'out-of-plane' reflections (see above, trees, poles), analysed by surveying the same line with different antenna orientations; this is suppressed by shielding. It is easy to think of the radar wave as a focused beam (the ray-path at right-angles to the wave) when in fact the radar wave as it travels into the subsurface is more like a figure of eight bubble, ovates-shaped at first, expanding and becoming both a single oval and distorted as it travels at different speeds into the ground. Thus lateral to the antennae, on or in the ground surface may be structures that cause reflections at ground level. The effect of these surface features can be diminished by altering the orientation of the antennae, or by shielding the above-ground portion of the antennae, such that the radio wave is focussed to penetrate the ground. GPR has found its best uses in imaging glaciers, sand deposits (river, non-saline coastal sands), aquifers (porous nature), archaeological features (moats, buried buildings, graves) and concrete/pavements.